# Magnetoimpedance studies in as quenched Fe73.5Si13.5B8CuV3−xAlNbx nanocrystalline ribbons

Venkatrao Chunchu and Markandeyulu G

Citation: Journal of Applied Physics **113**, 17A321 (2013); doi: 10.1063/1.4795800
View online: http://dx.doi.org/10.1063/1.4795800
View Table of Contents: http://scitation.aip.org/content/aip/journal/jap/113/17?ver=pdfcov
Published by the AIP Publishing



# Magnetoimpedance studies in as quenched $Fe_{73.5}Si_{13.5}B_8CuV_{3-x}AlNb_x$ nanocrystalline ribbons

Venkatrao Chunchu[a] and Markandeyulu G
*Advanced Magnetic Materials Laboratory, Department of Physics, Indian Institute of Technology Madras, Chennai 600036, India*

(Presented 16 January 2013; received 9 November 2012; accepted 12 December 2012; published online 21 March 2013)

Ribbons of $Fe_{73.5}Si_{13.5}B_8CuV_{3-x}AlNb_x$ ($x = 0$, 1.0, 1.5) alloys were prepared by melt-spun technique at the speed of 37 m/s. Crystalline phase derived from $Fe_3Si$, in an amorphous matrix was observed in all the ribbons. As cast nanocrystalline ribbons were obtained by controlling cooling rates while quenching. The average crystallite sizes was calculated using the Scherrer's equation to be 44 nm, 39 nm, and 35 nm in $x = 0$, $x = 1.0$, and $x = 1.5$ ribbons, respectively. Magnetoimpedance measurements were carried out using an LCR meter. Among the investigated samples ($x = 0$, 1.0, 1.5), the largest magnetoimpedance of 61% was obtained for $x = 1$ ribbon annealed at 100 °C for 15 min, at 4 MHz. © *2013 American Institute of Physics*. [http://dx.doi.org/10.1063/1.4795800]

## INTRODUCTION

Development of magnetic field sensors based on magnetoimpedance (*MI*) effect has drawn attention in recent years, because of the excellent sensitivity compared to the several other sensors that are developed using various magneto transport effects.[1] *MI* is mainly observed in soft magnetic materials such as amorphous and nanocrystalline wires and ribbons.[1–3]

It has been reported that Fe-based nanocrystalline materials are the most suitable candidates for magnetic field sensors, because of their excellent soft magnetic properties.[4] There are some reports on the enhancement of *MI* in nanocrystalline state compared to the amorphous state.[5,6] This kind of nanocrystalline materials can be obtained by two methods, viz., primary crystallization of the amorphous precursors[2,7] and direct quenching (by melt spinning) of the parent alloys at appropriate low wheel speeds.[8]

However, there are very few reports on *MI* studies on as quenched nanocrystalline ribbons. Dwevedi and Markandeyulu have reported on *MI* studies of amorphous and nanocrystalline (on annealing) $Fe_{73.5}Si_{13.5}B_8CuV_3Al$ and $Fe_{73.5}Si_{13.5}B_8CuV_{1.5}AlNb_{1.5}$ ribbons.[5] The *MI* values were found to be increased in the nanocrystalline state compared to amorphous ribbons. In this paper, structural and frequency dependence of *MI* effect of as quenched nanocrystalline $Fe_{73.5}Si_{13.5}B_8CuV_{3-x}AlNb_x$ ($x = 0$, 1.0, 1.5) ribbons are presented.

## EXPERIMENTAL DETAILS

The $Fe_{73.5}Si_{13.5}B_8CuV_{3-x}AlNb_x$ ($x = 0$, 1.0, 1.5) alloys were prepared by arc-melting the constituent elements of high purity (Transition metals—99.95% purity and B—99.9% purity) in argon atmosphere. The alloy was melted several times by turning it upside down, to ensure homogeneity. The weight loss after the melting was found to be less than 0.7%.

The ribbons were made by melt spinning technique at the speed of 37 m/s under argon atmosphere. The quality of the ribbon depends on argon gas pressure as well as the rotating speed of the drum. The X-ray powder diffraction (XRD) technique was employed to confirm the amorphous/crystalline nature and to study the different types of phases present in the ribbons. Transmission electron microscope (TEM) studies were carried out using Philips CM12 microscope under 120 kV accelerating voltage on the ion milled as cast ribbons. Ion milling was done for getting transparent regions. The coercivity measurements were carried out using Lakeshore 7410 Vibrating Sample Magnetometer with the electromagnet model EM10-HV. The field sensitivity of the instrument is 0.01 Oe. The *MI* measurements are performed on ribbons. Alternating current of amplitude of 10 mA was passed through the ribbons along their length. The steady magnetic field was applied along the length of the ribbon using a Helmholtz coil. The impedance measurements were done using a Hioki 3532 LCR meter. The frequency of the alternating current was varied between 500 kHz and 5 MHz for ribbons of length 5 cm. The dimensions of the ribbons used for the *MI* measurement were ($5 \times 0.195 \times 0.0028$) cm, ($5 \times 0.144 \times 0.0045$) cm, and ($5 \times 0.112 \times 0.0032$) cm for $x = 0$, $x = 1$, and $x = 1.5$, respectively. A DC magnetic field up to 100 Oe was applied to observe *MI*. The *MI* is defined as

$$\frac{\Delta Z}{Z}(\%) = \frac{Z(H) - Z(H_{max})}{Z(H_{max})} \times 100, \quad (1)$$

where $Z(H)$ is the impedance at a field $H$ and $Z(H_{max})$ is the impedance at the field at which it saturates.

## RESULTS AND DISCUSSION

Fig. 1 shows the XRD patterns of the as cast and annealed $Fe_{73.5}Si_{13.5}B_8CuV_{(3-x)}AlNb_x$ ($x = 0$, 1.0, 1.5) ribbons. The presence of crystalline phase derived from $Fe_3Si$ in an amorphous matrix was observed in all the ribbons. The average crystallite size was calculated using Scherrer

[a]Author to whom correspondence should be addressed. Electronic mail: venkatarao@physics.iitm.ac.in.

 

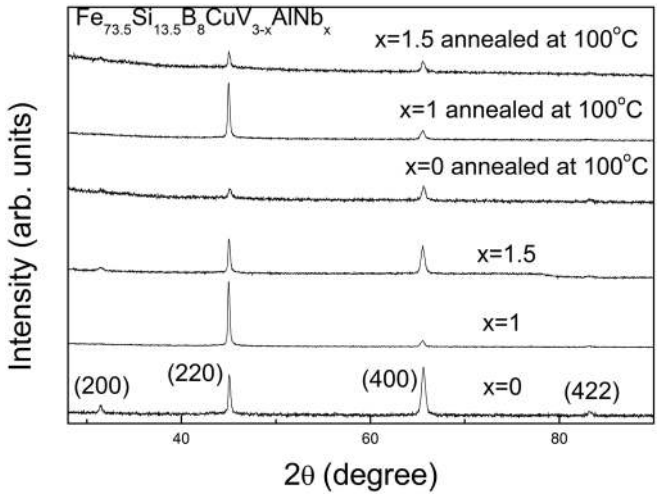


FIG. 1. XRD patterns of as cast and annealed $Fe_{73.5}Si_{13.5}B_8CuV_{(3-x)}AlNb_x$ (x = 0, 1.0, 1.5) ribbons.

equation. Crystallites of sizes 44 nm, 39 nm, 35 nm for the as cast and 30 nm, 42 nm, 55 nm for the annealed were obtained for x = 0, 1.0, and 1.5 ribbons, respectively. The change in average crystallite size upon annealing may be due to recrystallization, due to the presence of FCC-Cu particles, which act as heterogeneous nucleating sites for the Fe-Si primary crystals.[9]

Fig. 2 shows the TEM images and corresponding diffraction patterns of the as cast ribbons. Electron diffraction patterns from the x = 0 and 1.5 ribbons show diffuse rings, indicating the presence of amorphous phase. In addition to the central diffuse ring, another diffuse ring which encircles the strongest diffraction spot can be seen (Fig. 2). This sub-diffuse ring may be due to double diffraction, due to both crystalline and amorphous layers, indicating overlapping of the amorphous layer with the crystalline layer.[10] For the x = 1.0 ribbon (Fig. 2(b)), the diffuse rings are less intense compared to the x = 0 and 1.5 ribbons, probably due to reduction of amorphous phase within that area. Indexing of TEM electron diffraction patterns of ribbons x = 1.0 and x = 1.5 (Figs. 2(b) and 2(c)) revealed that the crystals stabilized in cubic FCC phase and the zone axis (electron beam direction) was along the [011] direction for x = 1.0 ribbon and along the [001] direction for x = 1.5 ribbon. Several spots were observed in the electron diffraction pattern for the x = 0 ribbon, probably due to irregular orientations of the grains in that area. Figs. 3–5 show the *MI* behavior with the applied field at different frequencies. In all the as cast ribbons, single peak behavior is observed, indicating the presence of longitudinal domains. An *MI* of 49%, the largest, was observed for x = 1 as cast ribbon at 3 MHz. For the x = 0 and x = 1.5 as cast ribbons, the largest *MI* values of 20% and 33% at 3 MHz (x = 0) and 2 MHz (x = 1.5), respectively, were observed. Dwevedi and Markandeyulu have reported *MI* studies on the as cast amorphous ribbons ($Fe_{73.5}Si_{13.5}B_8CuV_3Al$ and $Fe_{73.5}Si_{13.5}B_8$ $CuV_{1.5}AlNb_{1.5}$). The largest *MI* values of 7% (16%) and 15% (34%) have been reported for the as cast amorphous (annealed nanocrystalline) ribbons. The *MI* in amorphous material has been explained based on random anisotropy model,[11] by considering the grain size to be less than the exchange correlation length. Suzuki and Cadogan[12] extended the above to a mixture of amorphous and nanocrystalline phase. Bitoh *et al.*[13] have reported that the magneto-crystalline anisotropy in such mixtures as above not only depends on mean grain size but also on the grain size distribution. They have also proposed that the coercivity increases with the volume fraction of the coarse grains in the nanocrystalline material. In the present case, the coercivity values are found to be 0.6 Oe, 0.2 Oe, and 0.4 Oe for x = 0, 1.0, and 1.5 ribbons, respectively. The *MI* (Figs. 3–5) values in the as cast ribbons are seen to be small when the coercivity is large,

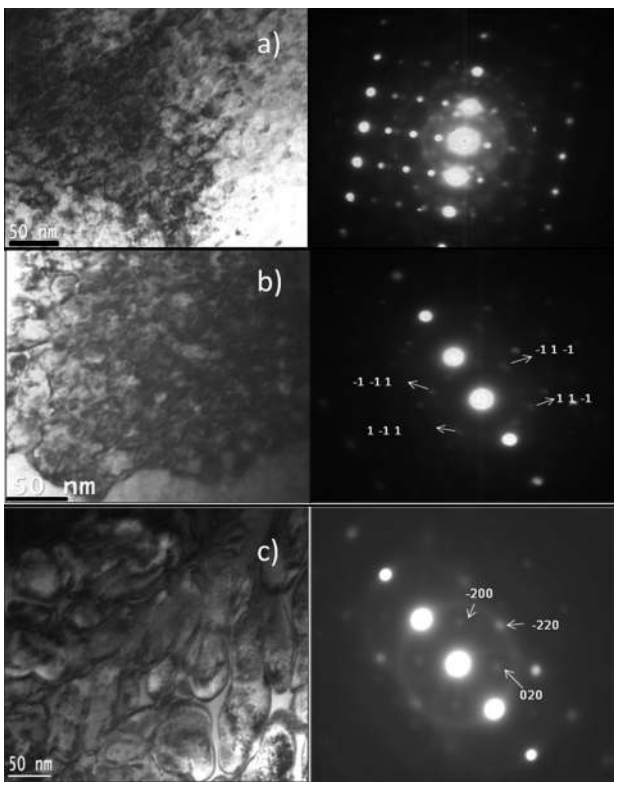


FIG. 2. TEM image (left) and diffraction pattern (right) of the as cast (a) x = 0, (b) x = 1.0, and (c) x = 1.5 ribbons.

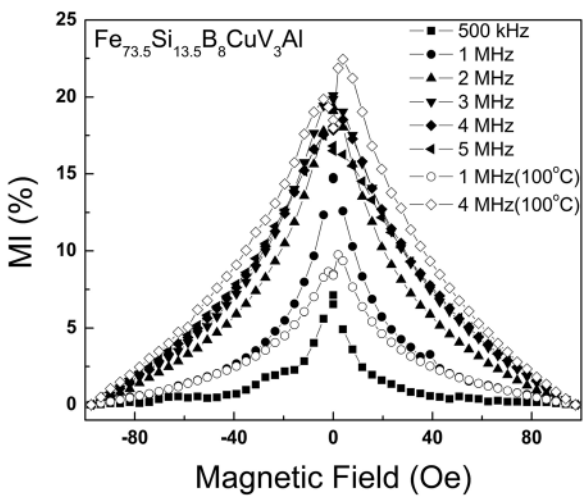


FIG. 3. Variation of *MI* with magnetic field for the as cast and annealed x = 0 ribbon of 5 cm length at different frequencies.

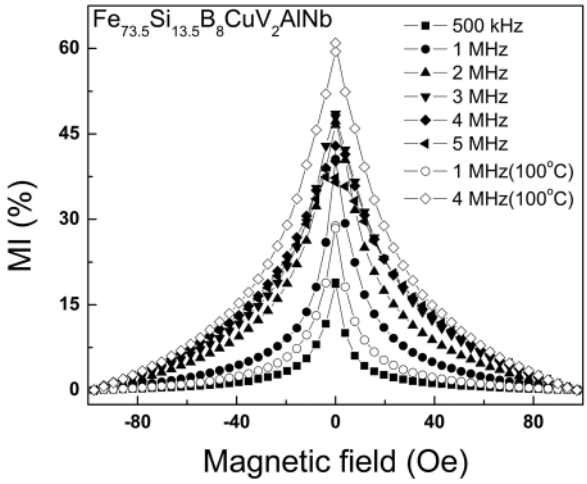


FIG. 4. Variation of *MI* with magnetic field for the as cast and annealed x = 1.0 ribbon of 5 cm length at different frequencies.

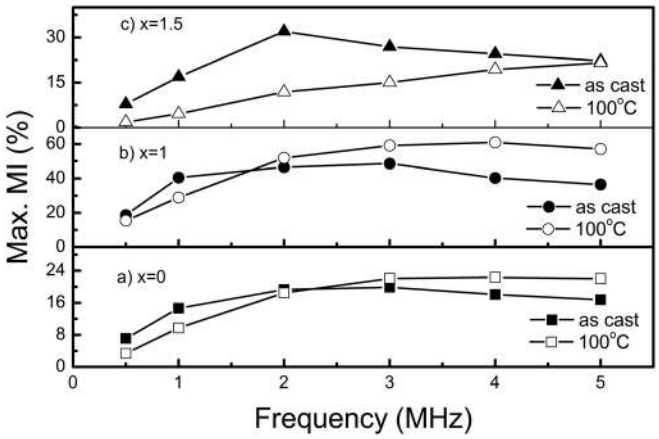


FIG. 6. Frequency variation of maximum *MI* for the as cast and annealed (a) x = 0, (b) x = 1, and (c) x = 1.5 ribbons.

confirming the relationship of *MI* to the grain size and distribution.

The *MI* is seen to increase with frequency, up to 3 MHz for the ribbons of x = 0 and x = 1.0 (Figs. 3 and 4) and up to 2 MHz for the x = 1.5 (Fig. 5) ribbon. This is due to the competition of decrease in permeability and an increase in skin effect, as the impedance is directly proportional to the square root of the product of transverse permeability and frequency.[14] The decrease of *MI* at higher frequencies may be due to the damping of domain wall motion. The largest *MI* of 61% was observed at 4 MHz for x = 1 ribbon annealed at 100 °C. For the x = 0 and x = 1.5 ribbons, the largest *MI* values of 22% and 22% at 4 MHz (x = 0) and 5 MHz (x = 1.5), respectively, were observed. For the annealed x = 0 ribbon, double peak behavior was observed, indicating the presence of transverse domains. There is also asymmetry in the *MI* profile for the x = 0 annealed ribbon. This may be due to non-uniform demagnetizing fields in the ribbon. The change in largest *MI* values of the annealed samples compared to as cast may be due to recrystallization of amorphous phase present in the as cast ribbons, which affects the grain size distribution and average grain size. For all the ribbons annealed at 100 °C, the largest *MI* has shifted towards the higher frequencies compared to the as cast ribbon (Fig. 6). This is probably due to decrease in the domain wall relaxation time, which produces shift in the initial permeability towards higher frequencies.[15]

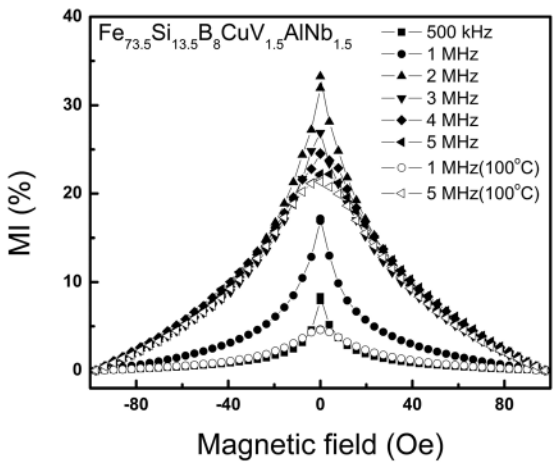


FIG. 5. Variation of *MI* with magnetic field for the as cast and annealed x = 1.5 ribbon of 5 cm length at different frequencies.

## SUMMARY AND CONCLUSIONS

The as cast nanocrystalline $Fe_{73.5}Si_{13.5}B_8CuV_{(3-x)}AlNb_x$ (x = 0, 1.0, 1.5) ribbons were prepared by melt-spun technique at a wheel speed of 37 m/s. The XRD and TEM studies showed that the as cast ribbons are crystallized in cubic (FCC) $Fe_3Si$ phase embedded in an amorphous matrix. Single peak behavior was observed in all the as cast ribbons, indicating the presence of longitudinal domains. Double peak behavior was observed for x = 0 annealed ribbon, indicating the presence of transverse domains. The largest *MI* of 61% was found for x = 1.0 ribbon annealed at 100 °C for 15 min. The frequency at which *MI* is the largest is seen to increase upon annealing.

[1]M. Knobel, M. L. Sánchez, C. Gómez-Polo, P. Marín, M. Vázquez, and A. Hernando, J. Appl. Phys. **79**, 1646 (1996).
[2]H. Lee, K.-J. Lee, Y.-K. Kim, T.-K. Kim, C.-O. Kim, and S.-C. Yul, J. Appl. Phys. **87**, 5269 (2000).
[3]C. Moron and A. Garcıa, J. Magn. Magn. Mater. **290**, 1085 (2005).
[4]M. E. McHenry, M. A. Willard, and D. E. Laughlin, Prog. Mater. Sci. **44**, 291 (1999).
[5]S. Dwevedi and G. Markandeyulu, Trans. Indian Inst. Met. **64**, 227 (2011).
[6]T. Sahoo, A. Chandra Mishra, V. Srinivas, T. K. Nath, M. Srinivas, and B. Majumdar, J. Appl. Phys. **110**, 083918 (2011).
[7]Y. Yoshizawa, S. Oguma, and K. Yamauchi, J. Appl. Phys. **64**, 6044. (1988).
[8]J. Hu, B. Li, H. Qin, and M. Jiang, Mater. Lett. **59**, 3069 (2005).
[9]K. Hono, Y. Zhang, A. P. Tsai, A. Inoue, and T. Sakurai, Scr. Metall. Mater. **36**, 909 (1995).
[10]H. Morikawa and M. Fujita, Thin Solid Films **359**, 61 (2000).
[11]R. Alben, J. J. Becker, and M. C. Chi, J. Appl. Phys. **49**, 1653 (1978).
[12]K. Suzuki and J. M. Cadogan, Phys. Rev. B **58**, 2730 (1998).
[13]T. Bitoh, A. Makino, A. Inoue, and T. Masumoto, Mater. Trans. **44**, 2011 (2003).
[14]T. Uchiyama, K. Mohri, L. V. Panina, and K. Furuno, IEEE Trans. Magn. **31**, 3182 (1995).
[15]J. M. Barandiarán, A. García-Arribas, J. L. Muñoz, G. V. Kurlyandskaya, and R. Valenzuela, J. Appl. Phys. **91**, 7451 (2002).